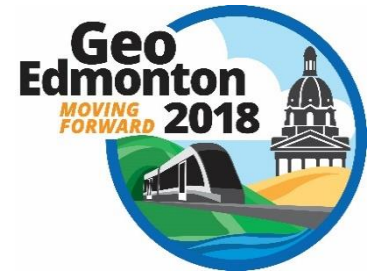


Numerical Modelling of Oblique Pipe–Soil Interaction in Dense Sand

MD Anan Morshed¹, Kshama Roy², Bipul Hawlader¹, & Ashutosh Sutra Dhar¹

¹Memorial University of Newfoundland, St. John's, NL, Canada

²Northern Crescent Inc., Calgary, Alberta, Canada



ABSTRACT

Pipe–soil interaction during large ground displacements is typically simulated using nonlinear soil springs aligned in three orthogonal directions with respect to the longitudinal axis of the pipeline. However, recent studies have indicated that in complex pipe–soil interaction events (e.g. lateral-vertical direction), assuming no interaction between the loads applied to the pipeline in different directions does not truly represent the field condition and therefore, an advanced numerical modelling is required. Finite element (FE) analysis of oblique (lateral-vertical) pipe–soil interaction for pipe buried in dense sand is presented in this paper. Two soil constitutive models, the Mohr–Coulomb (MC) model with constant angles of internal friction and dilation, and a Modified Mohr–Coulomb (MMC) model with pre-peak hardening, post-peak softening, density and confining pressure dependent friction and dilation angles, are considered. The FE analyses are performed using the Arbitrary Lagrangian Eulerian approach available in Abaqus/Explicit FE software. Results show a significant difference in the peak oblique resistance for different loading angles. Shear band formation due to strain localization for different loading angles is discussed from the simulations with both the MC and MMC models. FE results show that the MMC model can better simulate the oblique pipe–soil interaction event than the MC model.

RÉSUMÉ

L'interaction tuyau-sol lors de grands déplacements du sol est généralement simulée en utilisant des ressorts de sol non linéaires alignés dans trois directions orthogonales par rapport à l'axe longitudinal du pipeline. Cependant, des études récentes ont indiqué que dans les événements complexes d'interaction tuyau-sol (ex. Direction verticale-latérale), si aucune interaction entre les charges appliquées dans différentes directions ne représente vraiment l'état du champ, une modélisation numérique avancée est nécessaire. Champs obligatoires. L'analyse par éléments finis (EF) de l'interaction tuyau-sol oblique (latéral-vertical) pour un tuyau enfoui dans du sable dense est présentée dans cet article. Deux modèles constitutifs du sol, le modèle Mohr-Coulomb (MC) avec des angles constants de frottement interne et de dilatation, et un modèle Mohr-Coulomb (MMC) modifié avec durcissement pré-pic, adoucissement post-pic, densité et friction dépendante de la pression angles de dilatation, sont considérés. Les analyses FE sont effectuées en utilisant l'approche Eulérienne Lagrangienne Arbitraire disponible dans le logiciel Abaqus / Explicit FE. Les résultats montrent une différence significative dans la résistance oblique de crête pour différents angles de charge. La formation de la bande de cisaillement due à la localisation de la contrainte pour différents angles de charge est discutée à partir des simulations avec les modèles MC et MMC. Les résultats de FE montrent que le modèle MMC peut mieux simuler l'événement d'interaction oblique tuyau-sol que le modèle MC.

1 INTRODUCTION

Ground displacements—for example, landslides, fault movements and lateral spreading due to soil liquefaction—are some of the most dangerous geohazards that can impose a significant threat to buried pipelines. Ensuring safe and reliable operation of pipelines in the presence of these geohazards is therefore a prime concern for pipeline operators and regulatory agencies.

In current engineering practice, the modes of relative displacement between pipe and soil are generally categorized through three orthogonal springs in lateral, axial and vertical directions. In other words, the stiffness of the soil in three directions is independent of each other and therefore, the deformation in one direction has no effect on the others. However, the loading to the pipeline is not always aligned along one principal direction, and in most of the cases, combined (oblique) loading conditions are expected (Guo 2005; Cocchetti et al. 2009; Daiyan et al. 2011a). An oblique loading can be resulted from the combination of different directional loading, e.g. lateral-vertical, lateral-axial or axial-vertical loading. The

response of pipelines buried in dense sands and are subjected to oblique loading in the lateral-vertical direction is the focus of the present study.

Buried pipelines are generally installed into a trench. When the trench is backfilled with sand, the backfill material is generally in a loose to medium dense state. However, during the lifetime of a pipeline, the backfill sand might be densified due to traffic loads, nearby machine vibrations or seismic wave propagation (Kouretzis et al. 2013).

Several experimental (Audibert and Nyman 1978; Hsu 1996; Calvetti et al. 2004; di Prisco and Galli 2006; Merifield et al. 2008), theoretical (Nyman 1982; Cocchetti et al. 2009) and numerical (Calvetti et al. 2004; Yimsiri et al. 2004; Guo 2005; Pike and Kenny 2011; Daiyan et al. 2011a, 2011b; Farhadi Hikoei 2013; Jung et al. 2016) studies were conducted in the past to investigate the pipe–soil interaction in soil during an oblique movement. Very few studies among these were conducted in dense sand. For example, Nyman (1982) proposed an analytical approach whereas Cocchetti et al. (2009) used FE analysis to calculate the peak oblique soil resistance in dense sand.

However, they did not consider the post-peak softening behaviour of dense sand. In general, these studies showed the significance of considering the coupling between the loads in different directions on buried pipelines.

Physical tests are generally expensive and in most cases, it is not possible to conduct physical tests for a wide range of parameters. Numerical analysis has, therefore, gained significant attraction in recent years to analyze the complex pipe–soil interaction. One of the main challenges of numerical modelling of pipe–soil interaction is to choose an appropriate soil constitutive model. For example, although physical tests (Zhang et al. 2002; di Prisco and Galli 2006; Hsu et al. 2006) on oblique pipe–soil interaction in dense sand show post-peak softening behaviour, most of the previous numerical studies used the Mohr–Coulomb (MC) model that considers constant friction and dilation angles (Yimsiri et al. 2004; di Prisco and Galli 2006; Jung et al. 2016). The classical MC model cannot capture the post-peak softening behaviour of dense sand (Guo 2000; Roy et al. 2016). Furthermore, while using the MC model, in addition to the friction angle, the dilation angle also plays a significant role on lateral or uplift soil resistance of a pipeline. For anchor–soil interaction, Merifield and Sloan (2006) showed that, in extreme cases, the consideration of non-dilatant behaviour of dense sand (zero dilation angle) gave the ultimate lateral capacity of approximately half of the capacity of a soil model that satisfies the associated flow rule (dilation angle = friction angle). The above-mentioned study clearly shows the importance of the soil model in numerical modelling of pipe–soil interaction.

In the current design guidelines (e.g. ALA 2005, PRCI 2009) force–displacement relationships during pipe–soil interaction is defined by bilinear or hyperbolic functions. Therefore, the current guidelines fail to appropriately represent two important practical situations: (i) the post-peak degradation of the soil resistance to pipelines buried in dense sand, and (ii) the oblique loading conditions of the pipelines. The main objective of the present study is to present oblique (lateral-vertical) pipe–soil interaction modelling using an advanced soil model, named the modified Mohr–Coulomb (MMC) model, that can capture the post-peak degradation of soil resistance. A range of oblique loading angles (0 to 90°) is considered for a 300-mm diameter pipe embedded at 900 mm from the ground, surface to the centre of the pipe. The failure mechanisms of soil, i.e. the formation of shearing planes, are investigated to explain possible mechanisms involved in the force–displacement response.

2 FINITE ELEMENT FORMULATION

Two-dimensional FE analyses in plane strain condition are conducted to model the oblique (lateral-vertical) pipe–soil interaction. The pipe is modelled as a rigid body. Four-node, bilinear plane strain, reduced integration with an hourglass control element (CPE4R in Abaqus) is used for modelling the soil. The structured mesh is generated in Abaqus/CAE by zoning the soil domain. Figure 1 shows the typical FE mesh used in the present study. The soil is defined as an adaptive mesh domain with default Lagrangian type boundary regions, which results in new

smooth mesh with improved aspect ratios at a given interval.

The vertical faces of the soil domain are restrained from any lateral movement by using roller supports and the bottom face is restrained from the vertical and horizontal movement using hinge supports. No displacement boundary condition is applied at the top surface of the domain so that soil can move freely in the upward direction. The oblique angle (α) is defined as the angle of loading direction with the vertical, as shown in Fig. 1. The pipe is pulled in the oblique direction by defining both upward and lateral displacements during the loading step. For example, ~87 mm and ~50 mm displacements in the horizontal and vertical directions, respectively, are applied to the pipe centre to displace the pipe ~100 mm at an angle of 60° with the vertical.

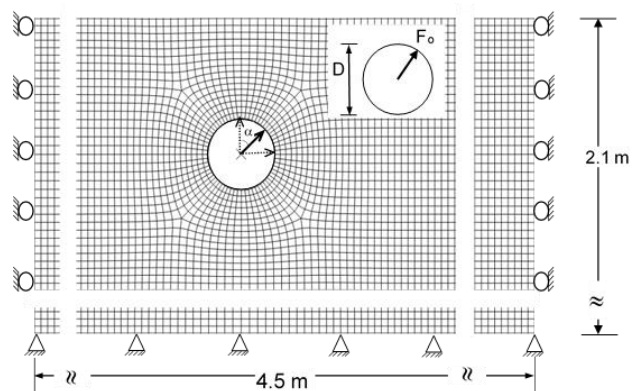


Figure 1. Typical FE mesh for $\tilde{H}=3$ and $D=300$ mm

To keep the pipe in the “wished-in-place” configuration, the centre of the pipe is placed at a distance H from the ground surface. The depth of the pipe is measured in terms of \tilde{H} ($= H/D$), which is termed the “embedment ratio.” The size of the soil domain is kept sufficiently large so that no boundary effects on the oblique resistance and soil failure mechanism are expected.

The interaction between pipe and soil is modelled using the contact surface approach available in Abaqus/Explicit. The Coulomb friction model is used, where the friction coefficient (μ) is defined by $\mu = \tan(\phi_\mu)$, ϕ_μ being the interface friction angle.

The authors are aware that the installation of the pipe may cause some disturbance to the soil closer to the pipe. However, the effect of such disturbance is not considered in the present study.

3 MODELLING OF SAND

Two soil constitutive models, the Mohr–Coulomb (MC) and a modified Mohr–Coulomb (MMC), are used in the present study. In the classical MC model, constant values of angles of internal friction (ϕ') and dilation (ψ) are defined. However, the MMC model proposed by Roy et al. (2016) considers the effects of pre-peak hardening, post-peak softening, density and confining pressure on mobilized angles of internal friction (ϕ') and dilation (ψ) of dense sand.

A detailed discussion of the MMC model, estimation of model parameters and comparison with the MC models are available in Roy et al. (2016, 2018a) and is not repeated

here. However, the constitutive equations are summarized in Table 1.

Table 1. Equations for Modified Mohr–Coulomb Model (MMC) (summarized from Roy et al. 2016)

Description	Eq. #	Constitutive Equations
Relative density index	(1)	$I_R = I_D(Q - \ln p) - R$, where $I_D = D_r(\%)/100$
Peak friction angle	(2)	$\phi'_p - \phi'_c = A_\psi I_R$
Peak dilation angle	(3)	$\psi_p = \frac{\phi'_p - \phi'_c}{K_\psi}$
Strain softening parameter	(4)	$\gamma_c^p = C_1 - C_2 I_D$
Plastic shear strain at ϕ'_p	(5)	$\gamma_p^p = \gamma_c^p \left(\frac{p}{p_a}\right)^m$
Mobilized friction angle at Zone–II	(6)	$\phi' = \phi'_{in} + \sin^{-1} \left[\left(\frac{2\sqrt{\gamma^p \gamma_p^p}}{\gamma^p + \gamma_p^p} \right) \sin(\phi'_p - \phi'_{in}) \right]$
Mobilized dilation Angle at Zone–II	(7)	$\psi = \sin^{-1} \left[\left(\frac{2\sqrt{\gamma^p \gamma_p^p}}{\gamma^p + \gamma_p^p} \right) \sin(\psi_p) \right]$
Mobilized friction angle at Zone–III	(8)	$\phi' = \phi'_c + (\phi'_p - \phi'_c) \exp \left[- \left(\frac{\gamma^p - \gamma_p^p}{\gamma_c^p} \right)^2 \right]$
Mobilized dilation angle at Zone–III	(9)	$\psi = \psi_p \exp \left[- \left(\frac{\gamma^p - \gamma_p^p}{\gamma_c^p} \right)^2 \right]$
Young's modulus	(10)	$E = K p_a \left(\frac{p}{p_a}\right)^n$

The soil parameters used in the present FE analysis are shown in Table 2. Note that the mesh size influences FE simulation results when softening behaviour of the soil is considered. However, this issue has not been discussed in the present study.

4 RESULTS

The FE model was first validated for two 1g model tests with 100-mm diameter pipe for pure lateral ($\bar{H} = 5.5$) and pure vertical loading ($\bar{H} = 3$) conditions, conducted by Trautmann (1983) and Cheuk et al. (2005, 2008), respectively. These tests were conducted in dense sand, having $D_r \sim 80\%$ for lateral loading (Trautmann 1983) and 92% for upward loading (Cheuk et al. 2005, 2008), respectively. Details of the validation of the FE model and performance of the MMC model can be found in Roy et al. (2016, 2018b) and are not repeated here due to the space limitation. For the present study, a 300-mm diameter pipe buried at $\bar{H}=3$ was pulled at different oblique angles (α) ranging from 0 to 90°, as shown in Fig. 1. The force–

displacement behaviour and the associated failure mechanism are discussed in the following sections. In the following sections, unless noted otherwise, the force–displacement curves are presented in normalized forms as $N_o (=F_o/\gamma HD)$ versus w/D , where F_o is the oblique resistance on the pipe per unit length (Fig. 1); H is the depth of the center of the pipe from the soil surface prior to pulling, γ is the dry unit weight of soil, and w is the oblique displacement. The peak value of N_o is defined as N_{op} , and the displacement required to reach to the peak is defined as w_p .

4.1 Force–displacement behaviour

Figure 2 shows the normalized force–displacement curves for $\alpha = 0$ to 90°. For $\alpha = 0 - 60^\circ$, N_o increases with w/D , reaches the peak (N_{op}) and then gradually decreases with w/D , which is primarily due to the strain-softening behaviour of dense sand. After a certain w/D , N_o becomes almost constant. However, for $\alpha = 75 - 90^\circ$, N_o increases with w/D , reaches point A, creating a plateau shape and

then increases again with w/D (Fig. 2). Note that for a certain α , the pipe was pulled out in the oblique direction, defining both horizontal and vertical displacements at the pipe reference point, as shown in Fig. 1. For example, for $\alpha = 90^\circ$, the pipe is displaced by defining the horizontal displacement while keeping the vertical displacement as zero. As the pipe cannot move upward, after reaching point A (Fig. 2), instead of decreasing, N_o starts to increase again with w/D . A similar reason governs the force–displacement behaviour for $\alpha = 75^\circ$, no post-peak softening after the peak. For further clarification, an additional FE analysis for $\alpha = 90^\circ$ has been conducted by applying a horizontal displacement at the pipe centre, however, the pipe is free to move in the vertical direction. The force–displacement behaviour obtained from this analysis is also plotted in Fig. 2 (broken line). A clear post-peak softening behaviour of the force–displacement curve after the peak is evident when the pipe is free to move in the vertical direction. Although most of the available physical test results on pure lateral loading (Trautmann 1983, Wijewickreme 2009) show a clear post-peak softening behaviour of the force–displacement curve, due to the ability of pipe to move vertically, the continuous increase of the force–displacement curve (i.e., no post-peak degradation), when the pipe was restrained vertically, was also obtained by Fenza (2016) in their physical test results on 219.1-mm diameter pipe buried in sand and pulled at $\alpha = 90^\circ$. Figure 2 also shows that the peak oblique resistance (N_{op}) is maximum for $\alpha = 90^\circ$ and minimum for $\alpha = 0$. Similar results were also found by Daiyan et al. (2011b) for their oblique pipe loading tests in dense sand.

Table 2. Parameters used in FE analyses

Parameters	Value
Pipe Diameter, D (m)	0.3
K	150
n	0.5
Atmospheric pressure, p'_a (kN/m ²)	100
v_{soil}	0.2
A_ψ	5
k_ψ	0.8
Initial angle of internal friction, ϕ'_{in} (°)	29
C_1	0.22
C_2	0.11
m	0.25
Critical state of friction angle, ϕ'_c (°)	35
Relative density, D_r (%)	80
Dry unit weight γ (kN/m ³)	17.7
Interface friction coefficient, μ	0.32
Embedment ratio, H/D	3
Cohesion, c' (kN/m ²)	0.1 ¹

¹A very small cohesion value is used to avoid the numerical issue although $c' = 0$ for sand.

To show the advantages of the MMC model, three FE simulations with the MC model were also conducted for $\alpha = 60^\circ$ using three sets of ϕ' and ψ values $\phi' = 45^\circ, \psi = 17^\circ$; $\phi' = 45^\circ, \psi = 0^\circ$ and $\phi' = 35^\circ, \psi = 0^\circ$.

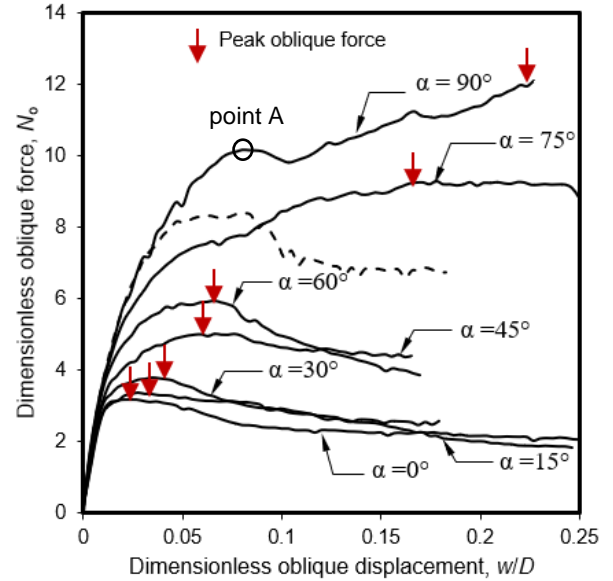


Figure 2. Dimensionless force vs displacement plot for different oblique angles

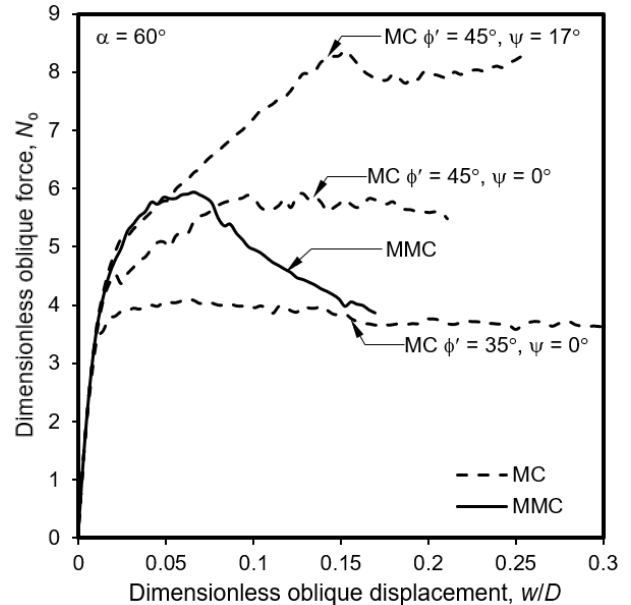


Figure 3. Dimensionless force vs displacement plot for both MC and MMC model

For the MC model, N_o increases with w/D , reaches a peak (N_{op}) and then remains almost constant (Fig. 3). As shown in Fig. 3, the dilation angle plays a significant role in the oblique resistance of pipeline. For the MC model with $\phi' = 45^\circ, \psi = 17^\circ$, N_{op} is significantly higher compared to $\phi' = 45^\circ, \psi = 0^\circ$. Furthermore, the peak oblique resistance with the MC model for $\phi' = 45^\circ, \psi = 17^\circ$ is ~33% higher than the peak oblique resistance obtained from the MMC model. Another key observation from Fig. 3 is that the simulations with the MC model do not show any post-peak degradation of N_o , as observed in the physical tests and FE simulations with the MMC model.

FE analyses are also conducted with the three sets of the MC model for a wide range of α ($= 0 - 90^\circ$) and the peak oblique resistance is plotted against α in Fig. 4. The peak oblique resistance obtained from the FE analysis with the MMC model is also plotted in Fig. 4 for further comparison. For the MC model, the difference in the peak oblique resistance for three sets of ϕ' and ψ values is higher for $\alpha = 90^\circ$ and the difference gradually decreases as α decreases (Fig. 4). In other words, the representative values of ϕ' and ψ also depend on α . For example, although $\phi' = 44^\circ$ and $\psi = 16^\circ$ gives N_{op} comparable to N_{op} obtained from the MMC model for $\alpha = 30^\circ$, the same mobilized values of $\phi' = 44^\circ$ and $\psi = 16^\circ$ do not necessarily give comparable N_{op} for $\alpha = 75^\circ$. Therefore, one must be extremely careful in choosing the representative values of ϕ' and ψ when using the MC model to calculate the oblique resistance. However, the MMC model does not require the representative values of ϕ' and ψ to be defined; rather, the MMC model requires ϕ'_c value, which can be easily obtained from typical laboratory tests.

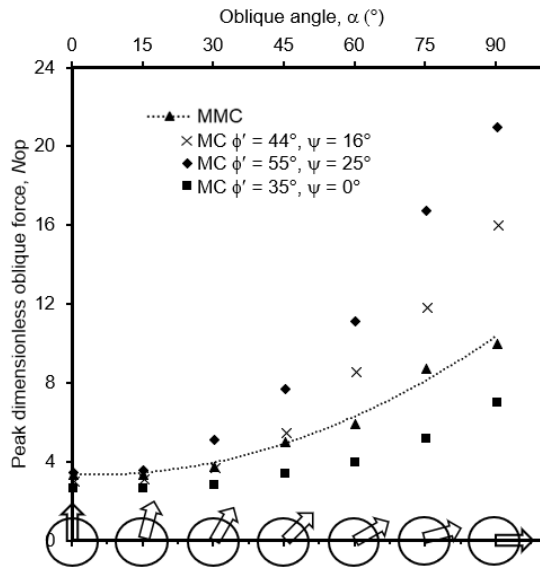


Figure 4. Peak dimensionless oblique force vs oblique angle for both MC and MMC models

Figure 5 shows the dimensionless horizontal vs vertical components of the reaction force for $\alpha = 0 - 90^\circ$ for both the MC and MMC models. For a certain α , the peak oblique resistance as well as the horizontal and vertical components of the oblique resistance can be calculated from Fig. 5. As mentioned earlier, the current design guidelines (e.g. ALA 2005 and PRCI 2009) consider only the pure peak lateral and vertical resistances and therefore, may not necessarily represent the oblique pipe-soil interaction events. The peak lateral and uplift resistances calculated from PRCI 2009 and ALA 2005 are also plotted in Fig. 5, for representative friction angle of dense sand. Figure 5 shows that one needs to be extremely careful in choosing the representative value of the friction angle for calculating the peak lateral and uplift resistances. Furthermore, the present study extends the

result to oblique resistances for a wide range of α that the current design guideline does not explicitly represent.

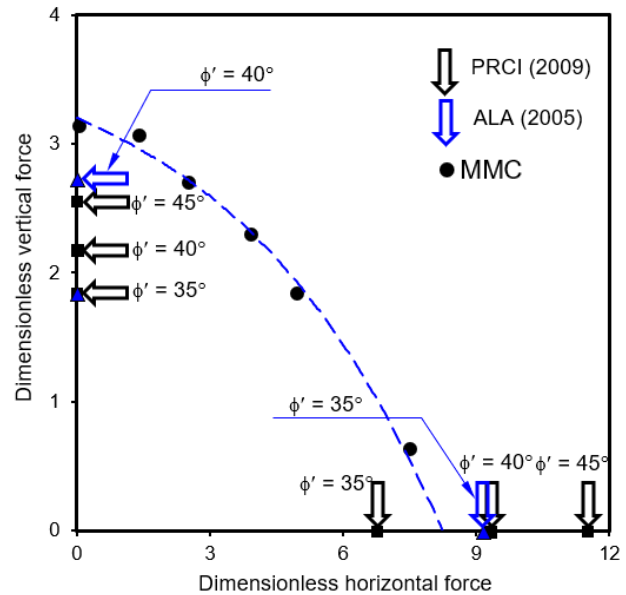


Figure 5. Dimensionless vertical force vs dimensionless horizontal force (MMC model)

4.2 Failure mechanism

The difference in the oblique resistance for different oblique angles (α) with the MMC model can be explained by the progressive development of shear bands. The plastic shear strains developed in soil at an oblique displacement of 50 mm ($w/D = 0.17$) for $\alpha = 60^\circ$ with the MMC model are shown in Fig. 6. As shown, significantly large plastic shear strains develop in some narrow zones at this level of oblique displacement. Three distinct shear bands, f_1, f_2 and f_3 are formed, as shown in Fig. 6. The shear bands in Fig. 6 are very similar to the model tests of Turner (2004) for lateral pipe-soil interaction in dense sand. In the MMC model, ϕ' and ψ are not constant but vary with plastic shear strain. The strain localization initiates at high values of ϕ' and ψ near the peak which eventually reduces to the critical state at moderate to large displacements. As the post-peak softening of stress-strain behaviour is not considered, the MC model cannot simulate the degradation of N_o after the peak, as shown in Fig. 3.

Broken lines through the highly concentrated γ^p zone (Fig. 6) are drawn for further investigation of the location of the shear bands for different α . As in Fig. 6, the locations of the shear bands are also obtained for $\alpha = 45^\circ$ and plotted in Fig. 7 for $w/D=0.17$. Figure 7 shows that the inclination of the shear band with the horizontal decreases with an increase in α , which results in higher resistance for higher α .

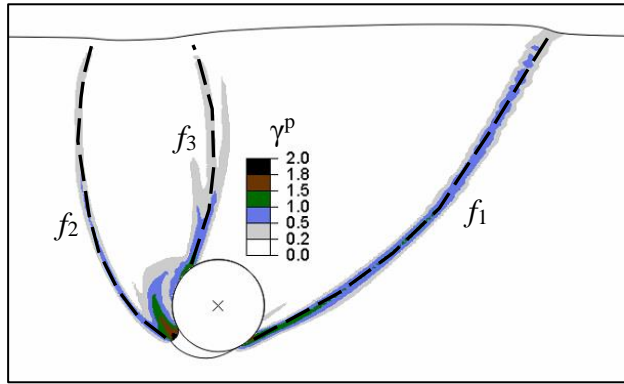


Figure 6. Formation of the shear band for the MMC model ($\alpha = 60^\circ$, $w/D = 0.17$)

The size of the failure wedge for $\alpha = 60^\circ$ is higher than that of $\alpha = 45^\circ$ and therefore, the oblique resistance is higher for $\alpha = 60^\circ$. For a similar reason, $\alpha = 0^\circ$ results in the lowest resistance whereas $\alpha = 90^\circ$ results in highest resistance. However, the oblique resistance is a function of not only the size of the failure wedge but also the mobilized ϕ' and ψ values along the shear band. The MMC model can successfully capture both features of the oblique pipe–soil interaction.

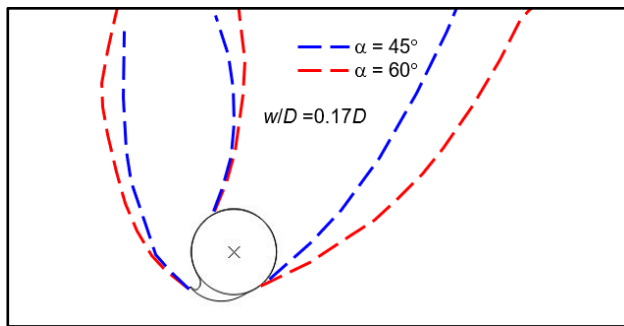


Figure 7. Formation of the shear band for the MMC model for $\alpha = 45^\circ$ and 60°

5 CONCLUSIONS

Finite element analysis of oblique pipe–soil interaction (lateral–vertical) is conducted for a 300-mm diameter pipe buried at 750 mm (from the ground surface to the centre of pipe) for a wide range of oblique angles ranging from 0° to 90° . The analyses are conducted using Abaqus/Explicit FE software. Recognizing the fact that the constitutive model of sand influences the calculated resistance, a comparative study is performed using the built-in Mohr–Coulomb model in Abaqus and a modified Mohr–Coulomb (MMC) model. The progressive formation of shear bands and their relation to the force–displacement response is carefully examined. Results show that the MMC model can better simulate the oblique pipe–soil interaction event than the built-in MC model. The analysis presented in the paper is only for one geometry and set of soil properties. Further study of the effects of depth of embedment, pipe diameter and soil parameters is required.

6 ACKNOWLEDGEMENTS

The work presented in this paper has been supported by the Natural Sciences and Engineering Research Council of Canada (NSERC), Petroleum Research Newfoundland & Labrador and Mitacs.

7 REFERENCES

- American Lifelines Alliance (ALA) 2005. *Guidelines for the Design of Buried Steel Pipe*. <<https://www.americanlifelinesalliance.com/pdf/Update061305.pdf>> (Mar. 13, 2018).
- Audibert, J.M. and Nyman, K.J. 1977. Soil restraint against horizontal motion of pipes. *Journal of the Geotechnical Engineering Division*, 103(10): 1119–1142.
- Calvetti, F., di Prisco, C. and Nova, R., 2004. Experimental and numerical analysis of soil–pipe interaction. *Journal of geotechnical and geoenvironmental engineering*, 130(12): 1292–1299.
- Cheuk, C. Y., White, D. J. and Bolton, M. D. 2005. Deformation mechanisms during the uplift of buried pipelines in sand. *Proc., 16th -International Conference on Soil Mechanics and Geotechnical Engineering*, Osaka, 1685–1688.
- Cheuk, C. Y., White, D. J. and Bolton, M. D. 2008. Uplift Mechanisms of Pipes Buried in Sand. *Journal of Geotechnical and Geoenvironmental Engineering*, 134(2): 154–163.
- Cocchetti, G., di Prisco, C., Galli, A., & Nova, R. 2009. Soil–pipeline interaction along unstable slopes: a coupled three-dimensional approach. Part 1: Theoretical formulation. *Canadian Geotechnical Journal*, 46(11): 1289–1304.
- Daiyan, N., Kenny, S., Phillips, R. and Popescu, R. 2011a. Investigating pipeline–soil interaction under axial–lateral relative movements in sand. *Canadian Geotechnical Journal*, 48(11): 1683–1695.
- Daiyan, N., Kenny, S., Phillips, R. and Popescu, R. 2011b. Numerical investigation of axial-vertical and lateral-vertical pipeline/soil interaction in sand. *14th Pan-American Conference on Soil Mechanics and Geotechnical Engineering*. Toronto, Ontario, Canada.
- Farhadi Hikoei, B. 2013. Numerical modeling of pipe-soil interaction under transverse direction. Doctoral thesis, University of Calgary.
- Fenza, G. 2016. Experimental and numerical investigations to assess the behaviour of a buried pipeline in areas with high geological instability. Doctoral thesis, University of Calgary.
- Guo, P. 2000. Modelling granular materials with respect to stress-dilatancy and fabric: A fundamental approach. PhD Thesis, University of Calgary.
- Guo, P. 2005. Numerical modeling of pipe–soil interaction under oblique loading. *Journal of Geotechnical and Geoenvironmental Engineering*, 131(2): 260–268.
- Hsu, T.W. 1996. Soil restraint against oblique motion of pipelines in sand. *Canadian geotechnical journal*, 33(1): 180–188.

- Hsu, T.W., Chen, Y.J. and Hung, W.C. 2006. Soil restraint to oblique movement of buried pipes in dense sand. *Journal of Transportation Engineering*, 132(2): 175–181.
- Jung, J.K., O'Rourke, T.D. and Argyrou, C. 2016. Multi-directional force–displacement response of underground pipe in sand. *Canadian Geotechnical Journal*, 53(11): 1763–1781.
- Kouretzis, G.P., Sheng, D. and Sloan, S.W. 2013. Sand–pipeline–trench lateral interaction effects for shallow buried pipelines. *Computers and Geotechnics*, 54: 53–59.
- Merifield, R.S. and Sloan, S.W. 2006. The ultimate pullout capacity of anchors in frictional soils. *Canadian Geotechnical Journal*, 43(8): 852–868.
- Merifield, R., White, D.J. and Randolph, M.F. 2008. The ultimate undrained resistance of partially embedded pipelines. *Géotechnique*, 58(6): 461–470.
- Nyman, K.J., 1982. Soil response against the horizontal-vertical motion of pipes. *American Society of Civil Engineers*.
- Pike, K. and Kenny, S. 2011, January. Advancement of CEL procedures to analyze large deformation. In *Offshore Technology Conference*.
- PRCI (2009). Guidelines for constructing natural gas and liquid hydrocarbon pipelines through areas prone to landslide and subsidence hazards. Pipeline Research Council International.
- Roy, K., Hawlader, B.C., Kenny, S. and Moore, I. 2016. Finite Element Modeling of Lateral Pipeline–Soil Interactions in Dense Sand, *Canadian Geotechnical Journal*, 53(3): 490–504.
- Roy, K., Hawlader, B.C., Kenny, S. and Moore, I. 2018a. Upward Pipe–Soil interaction for shallowly buried pipelines in dense sand, *Journal of Geotechnical and Geoenvironmental Engineering*, ASCE (In press)
- Roy, K., Hawlader, B.C., Kenny, S. and Moore, I. 2018b. Lateral Resistance of Pipes and Strip Anchors Buried in Dense Sand. *Canadian Geotechnical Journal* (In press, published online on March 22, 2018)
- Trautmann, C. 1983. Behavior of pipe in dry sand under lateral and uplift loading. PhD thesis, Cornell University, Ithaca, NY.
- Turner, J.E. 2004. Lateral force-displacement behavior of pipes in partially saturated sand. M.S. Thesis, Cornell University, Ithaca, NY.
- Wijewickreme, D., Karimian, H. and Honegger, D. 2009. Response of buried steel pipelines subjected to relative axial soil movement. *Canadian Geotechnical Journal*, 46(7): 735–752.
- Yimsiri, S., Soga, K., Yoshizaki, K., Dasari, G.R. and O'Rourke, T.D. 2004. Lateral and upward soil-pipeline interactions in sand for deep embedment conditions. *Journal of Geotechnical and Geoenvironmental engineering*, 130(8): 830–842.
- Zhang, J., Stewart, D.P. and Randolph, M.F. 2002. Modeling of shallowly embedded offshore pipelines in calcareous sand. *Journal of Geotechnical and Geoenvironmental engineering*, 128(5): 363–371.